International Journal of Sciences and Techniques of Automatic control & computer engineering
IJ-STA, Volume 9, N°1, December 2015, pp 2026–2034.

A Stability Analysis of Simultaneous Estimation of Speed and Stator Resistance for Sensorless IRFOC Induction Motor Drives

M. Jouili, Y. Agrebi, Y. Koubaa, and M. Boussak, *Senior Member, IEEE*

***Abstract*— This paper presents stability analysis of simultaneous speed and stator resistance estimators for sensorless indirect rotor flux oriented control (IRFOC) induction motor (IM) drives. Design of the observer feedback gain to guarantee stability, is proposed. Closed-loop control systems of the independent use of the two estimators are developed. All gains of the adaptive PI controllers, based on Root-Locus method, are chosen to allow good tracking performance and fast dynamic response. Performance of the Luenberger State Observer (LSO) using the proposed feedback gain and adaptive PI controller gains, with a indirect rotor flux oriented control (IRFOC) induction motor (IM) drives, is verified by experimental results. The results show a good improvement in both the convergence and stability, which support the validity of the proposed analysis.**

***Keywords*—IRFOC, Sensorless control, Simultaneous estimation, feed-forward decoupling, Luenberger State Observer (LSO).**

NOMENCLATURE

v_{qs} , v_{ds}	*q, d*-axis stator voltage components.
i_{qs} , i_{ds}	*q, d*-axis stator current components.
Φ_{ds} , Φ_{qs}	*d, q*-axis stator flux components.
R_r , R_s	Rotor and stator winding resistance.
L_r , L_s	Rotor and stator self-inductance.
M	Mutual inductance.
n_p	Number of pole pairs.
ω_r , ω_s	Rotor and synchronous angular speed.
ω_{sl}	Slip angular speed $\omega_s - \omega_r$.
T_l , T_e	Load and Electromagnetic torque.
J	Moment of inertia.
f	Friction constant.
τ_r , τ_s	Rotor and stator time constant.
$k_{\omega p}$, $k_{\omega i}$	Proportional and Integral gain of the IP speed controller.
k_{ip} , k_{ii}	Proportional and Integral gain of the PI current controller.
σ	Total leakage constant.
*, ^	Reference and estimated value.

M. Jouili, Y. Agrebi and Y. Koubaa are with Laboratory of Sciences and Techniques of Automatic control & computer engineering (Lab-STA), National School of Engineering of Sfax – University of Sfax – B.P. 1173 – Sfax – Tunisia (e-mail: mabrouk.jouili@gmail.com, agrebi69@yahoo.fr, yassine.koubaa@enis.rnu.tn)

M. Boussak is with Laboratoire des Sciences de l'Information et des Systèmes (LSIS) – UMR CNRS 7296 – Ecole Centrale Marseille (ECM) – 38 rue Frédéric-Joliot Curie –13451 Marseille Cedex 20 – France, (e-mail: mohamed.boussak@centrale-marseille.fr)

I. INTRODUCTION

MODERN industrial spectra show a growing interest in the use of motor drive systems. Such systems are fed by pulse-width modulation voltage source inverters (PWM-VSIs). They are broadly utilized for variable-speed industrial operations; for instance, aeronautics, railway traction and robotics.

Researchers have been seeking to improve the above-mentioned qualities through the ingenious and intricate control techniques resting on the FOC. Such methods control both the amplitude and the ac-excitations phase. In the same context, in order to know the rotor speed of the high-performance IM drive, the vector control method has also been used. The incremental encoder is the most widespread positioning transducer and the most reliable in modern industry [1, 2]. It is the most likely to provide such information.

Actually, when using this sensor, a long list of problems may arise. Indeed, among these problems we can cite the increasing cost, abundance of electronics, lack of reliability, and complex assembling. For example, the motor drives and high speed drives in harsh environment are cases in point. What is more, weight and size increase, and increase in electrical susceptibility are parts of the list of these problems.

The problem of eliminating transducers has recently caught the attention of researchers. To remedy this problem, however, many approaches have been dedicated to the evaluation of the rotor velocity and / or position. When examining the newly published literature, we discover the extent to which researchers have been interested in the design of the sensorless vector control IM drives. Such techniques are, undeniably, founded on these schemes:

Model Reference Adaptive System (MRAS): [3, 4].
Kalman Filters (EKF): [5, 6].
Neuronal networks observers and fuzzy logic [7-9].
Luenberger Observer (LO): [10, 11].

As a matter of fact, to apply some of these approaches, particularly modified machines, the injection of disturbance signals and the use of a IM model are needed. Practically speaking, the other velocity estimation methods via IM

This paper was recommended for publication in revised form by the Editor Staff.
Edition: CPU of Tunis, Tunisia, ISSN: 1737-7749

model supplied by the stator quantities depend on the parameter; hence, the errors of the parameter can negatively affect the speed control feasibility. Accordingly, to get a feasible sensorless vector control drive, we have to adapt the parameters.

When speed is set at its lowest levels, we notice that the IRFOC of the IM drive is highly sensitive to the exact value of the stator resistance in the rotor flux. To solve the difficulty, we have to tune the stator resistance variation of the IM online so as to keep the active performance of the sensorless IRFOC drive. To evaluate the rotor velocity and the stator resistance, many researchers studying the drives with no shaft transducers [12, 14] have lately been developed. These works have laid emphasis on the use of various approaches. Almost all of these methods need extra-sensors that are not widely utilized in IRFOC drive; thus, cost and involvedness may impede practice.

This research is intended to contribute to the question of speed of the sensorless IRFOC of IM drive with a stator resistance tuning. In fact, the considered observer, which is based on the estimated and measured stator currents and the estimated rotor flux, estimates the rotor speed and the stator resistance. In other words, this observer is to simultaneously estimate the rotor velocity, the rotor flux, the stator resistance, and the stator currents. In an attempt to obtain a sequential and simple design of the observer, the singular disturbance theory is applied. Still, the flux observer stability is realized by the Lyapunov theory. Then, we fully describe and justify the suggested algorithm and we test its performances by simulations. Despite the existence of the related algorithms, these contributions are thought to be innovative. Initially, we analyze the active and stable state performances and check the outstanding behavior in most instances. Next, we employ the rotor flux oriented control and develop an overall framework.

This paper is organized as follows: section 2 is a succinct review of the IRFOC of the IM drives. Section 3 is dedicated to the description of the feed-forward decoupling controller. In Section 3, we depict the design procedure which is suggested with the intention of estimating the rotor rapidity and the rotor resistance in a simultaneous way. The procedure design proposed to determine the gains of the regulators, the speed estimators and the stator resistance is described in Section 4. Thereafter, we illustrate the experimental results in section 5. Lastly, the paper is ended up with some comments and conclusions in Section 6.

II. Rotor Flux Orientation Strategy

When referring to the IRFOC, the rotor flux vector is aligned with d-axis. It sets the rotor flux to be regular equal to the rated flux. This means that $\Phi_{dr} = \Phi_r$ and $\Phi_{qr} = 0$.

A. IM Model

The IM active model can be shown along with the ordinary components *q-axis* and d-*axis* in a synchronous rotating framework:

$$v_{ds} = \sigma L_s \left(p + \frac{1}{\sigma\tau_s} + \frac{1-\sigma}{\sigma\tau_r} \right) i_{ds} - \sigma L_s \omega_s i_{qs} - \frac{M}{L_r \tau_r} \Phi_r \tag{1}$$

$$v_{qs} = \sigma L_s \left(p + \frac{1}{\sigma\tau_s} + \frac{1-\sigma}{\sigma\tau_r} \right) i_{qs} + \sigma L_s \omega_s i_{ds} + \frac{M}{L_r} \omega \Phi_r \tag{2}$$

$$\Phi_r = \frac{M}{1+\tau_r p} i_{ds} \tag{3}$$

$$T_e = n_p \frac{M}{L_r} i_{qs} \Phi_r \tag{4}$$

$$\omega_{sl} = \frac{M}{\tau_r \Phi_r} i_{qs} \tag{5}$$

Where $\omega_{sl} = \omega_s - \omega_r$; $\tau_r = \frac{L_r}{R_r}$; $\tau_s = \frac{L_s}{R_s}$ and $\sigma = 1 - \frac{M^2}{L_s L_r}$.

We can assume that if the rotor flux is maintained constant, the *q-axis* current can be restricted by the torque. In this respective, the relation between the electrical angular speed motor and the electromagnetic torque equation can be expressed by :

$$J \frac{d\omega_r}{dt} + f \omega_r = n_p (T_e - T_l) \tag{6}$$

B. Feed-forward decoupling controller

The d-axis and the q-axis voltage equations are combined by these expressions $-\left(\sigma L_s \omega_s i_{qs} + \frac{M}{L_r \tau_r} \Phi_r \right)$ and $\sigma L_s \omega_s i_{ds} + \frac{M}{L_r} \omega \Phi_r$.

$$v_d = v_{ds} + E_d = \sigma L_s \left(p + \frac{1}{\sigma\tau_s} + \frac{1-\sigma}{\sigma\tau_r} \right) i_{ds} \tag{7}$$

$$v_d = v_{ds} + E_d = \sigma L_s \left(p + \frac{1}{\sigma\tau_s} + \frac{1-\sigma}{\sigma\tau_r} \right) i_{ds} \tag{8}$$

Where $E_d = \left(\sigma L_s \omega_s i_{qs} + \frac{M}{L_r \tau_r} \Phi_r \right)$ and $E_q = \sigma L_s \omega_s i_{ds} + \frac{M}{L_r} \omega \Phi_r$; E_q and E_d are, respectively, the *q*- and *d*-back electromotive force (EMF).

The system equations (7) and (8) yield the transfer functions of the stator currents :

$$G_d(p) = G_q(p) = \frac{K_c}{1+\tau_c p} \tag{9}$$

Where $K_c = \frac{1}{R_s}$ is a gain and $\tau_c = \sigma\tau_s$ is a time constant.

The closed-loop current transfer function is

$$\frac{i_{ds}(p)}{i_{ds}^*(p)} = \frac{i_{qs}(p)}{i_{qs}^*(p)} = \frac{\omega_n^2}{p^2 + 2\xi\omega_n p + \omega_n^2} \left(1 + \frac{K_{ip}}{K_{ii}} p \right) \tag{10}$$

This allows us to write

$$\begin{cases} K_{ip} = \dfrac{2\xi\tau_c \dfrac{k}{t_r} - 1}{K_c} \\ K_{ii} = \dfrac{\tau_c}{K_c} \left(\dfrac{k}{t_r} \right)^2 \end{cases} \tag{11}$$

Where $\omega_n = \sqrt{\frac{K_c K_{ii}}{\tau_c}}$ and $\xi = \frac{1 + K_c + K_{ip}}{2\omega_n \tau_c}$.

ξ and ω_n respectively signify the damping ratio and the natural frequency.

For any damping ratio, the second-order systems give a steady value for $\omega_n t_r = k$.

For instance, if we have a damping ratio $\xi = 1$, we will get $\omega_n t_r \approx 4.75$.

The speed control is ensured by an IP controller.

$$\frac{\omega_r(p)}{\omega_r^*(p)} = \frac{\omega_n^2}{p^2 + 2\xi\omega_n p + \omega_n^2} \tag{12}$$

With $\omega_n^2 = \frac{n_p K_{vi} K_{vp} \lambda}{J}$; $2\xi\omega_n = \frac{f + n_p K_{vp} \lambda}{J}$ and $\lambda = \frac{T_e}{\omega_{sl}} = n_p \frac{\Phi_r^2}{R_r}$

Where K_{vi} and K_{vp} indicate the integral and proportional the gains of the *IP* speed regulator

$$\begin{cases} K_{vp} = \dfrac{2J\xi\left(\dfrac{k}{t_r}\right) - f}{n_p \lambda} \\ K_{vi} = \dfrac{J\left(\dfrac{k}{t_r}\right)^2}{n_p \lambda K_{vp}} \end{cases} \tag{13}$$

III. Adaptive Luenberger Observer

A. Flux observer of IM

The following rotating reference frame is most likely to describe the induction motor state model

$$\begin{cases} \dot{x}(t) = \mathbf{A}x(t) + \mathbf{B}v_s(t) \\ y(t) = \mathbf{C}x(t) \end{cases} \tag{14}$$

The adaptive flux observer is defined by the following state representation

$$\begin{cases} \dot{\hat{x}}(t) = \hat{\mathbf{A}}\hat{x}(t) + \mathbf{B}v_s(t) + \mathbf{L}\left[y(t) - \mathbf{C}\hat{x}(t)\right] \\ \hat{y}(t) = \mathbf{C}\hat{x}(t) \end{cases} \tag{15}$$

Where $\hat{x} = \begin{bmatrix} \hat{i}_{ds} & \hat{i}_{qs} & \hat{\Phi}_{dr} & \hat{\Phi}_{qr} \end{bmatrix}^T$; $x = \begin{bmatrix} i_{ds} & i_{qs} & \Phi_{dr} & \Phi_{qr} \end{bmatrix}^T$;

$\hat{y} = \begin{bmatrix} \hat{i}_{ds} & \hat{i}_{qs} \end{bmatrix}^T$; $y = \begin{bmatrix} i_{ds} & i_{qs} \end{bmatrix}^T$; $v_s(t) = \begin{bmatrix} v_{ds} & v_{qs} \end{bmatrix}^T$

$$\mathbf{A} = \begin{bmatrix} -\gamma\mathbf{I_2} + \omega_r\mathbf{J} & \dfrac{1}{\sigma L_s \tau_r}\mathbf{I_2} - \dfrac{1}{\sigma L_s}\omega_r\mathbf{J} \\ -R_s\mathbf{I_2} & \mathbf{O_2} \end{bmatrix}; \mathbf{B} = \begin{bmatrix} \dfrac{1}{\sigma L_s}\mathbf{I_2} \\ \mathbf{I_2} \end{bmatrix};$$

$\mathbf{C} = \begin{bmatrix} \mathbf{I_2} & \mathbf{O_2} \end{bmatrix}$; $\mathbf{I_2} = \begin{bmatrix} 1 & 0 \\ 0 & 1 \end{bmatrix}$; $\mathbf{J} = \begin{bmatrix} 0 & -1 \\ 1 & 0 \end{bmatrix}$; $\mathbf{O_2} = \begin{bmatrix} 0 & 0 \\ 0 & 0 \end{bmatrix}$;

$\gamma = \frac{1}{\sigma L_s}\left(R_s + \frac{M^2}{L_r \tau_r}\right)$ and $\delta = \frac{M}{\sigma L_s L_r}$.

L denote the observer gain matrix which is selected for the stability of the system.

B. Luenberger State Observer Gain Design

To guarantee the disappearance of the evaluation error above time for each $\tilde{x}(0)$, we have to choose the observer gain matrix L so that (A-LC) is asymptotically stable. Indeed, we choose the observer gain matrix so that each the eigenvalues of (A-LC) have real negative parts. Additionally, to make every varieties of speed stable, we have to choose the observer poles proportional to the motor poles. If the IM poles are given by λ_{IM}, the observer poles λ_{LO} are designated as

$$\lambda_{LO} = k_p \lambda_{IM} \tag{16}$$

It is realized by specifying the observer matrix L in a particular representation

$$\mathbf{L} = \begin{bmatrix} l_1\mathbf{I_2} + l_2\mathbf{J} \\ l_3\mathbf{I_2} + l_4\mathbf{J} \end{bmatrix} = \begin{bmatrix} \mathbf{L_1} \\ \mathbf{L_2} \end{bmatrix} \tag{17}$$

To decide the eigenvalues of the matrix A, we employ:

$$\lambda_{IM}^2 + (a+b)\lambda_{IM} + (a - \delta c)b = 0 \tag{18}$$

To have the equation simplified, we have to define

$$a = \gamma I_2 \; ; \; b = \frac{1}{\tau_r} I_2 - \hat{\omega}_r J \text{ and } c = \frac{M}{\tau_r}$$

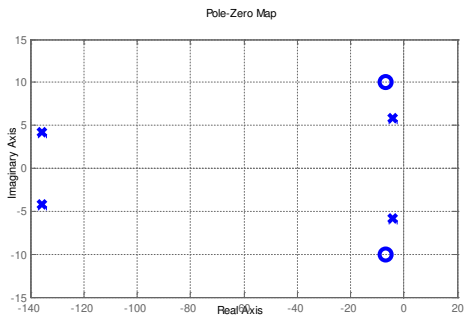
The matrix characteristic equation (A-LC) is

$$\lambda_{LO}^2 + (a + b - L_1)\lambda_{LO} + ((a - \delta c) - (L_1 + \delta L_2))b = 0 \tag{19}$$

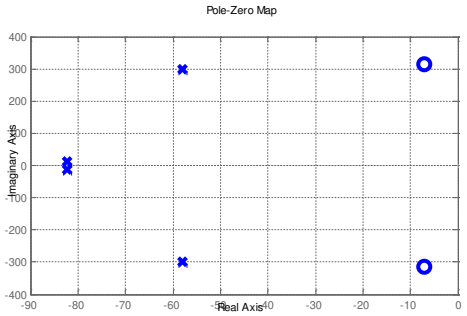
The substitution of Eq. (16) in (19) gives

$$k_p^2 \lambda_{IM}^2 + k_p(a + b - L_1)\lambda_{IM} + ((a - \delta c) - (L_1 + \delta L_2))b = 0 \tag{20}$$

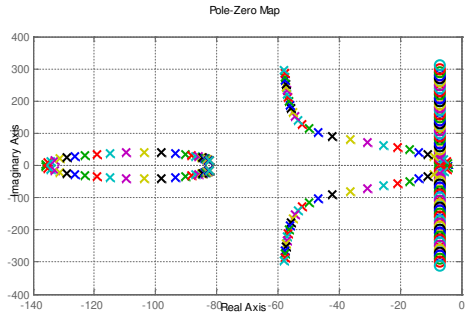
The following results are obtained by identifying Eq. (20) and $k_p^2 * (18)$



(a)



(b)



(c)

Fig. 1. Evolution of the system poles and zeros for different values of the speed ((a) speed of 5 rpm, (b) speed of 157 rpm and (c) speed of 0 to 157 rpms with a step of 5 rpm).

$$\begin{cases} l_1 = \left(1 - k_p\right)\left(\gamma' + \dfrac{1}{\tau_r}\right) \\ l_2 = \left(k_p - 1\right)\hat{\omega}_r \\ l_3 = \dfrac{1}{\delta}\left(k_p^2 - 1\right)\left(\gamma' - \delta\dfrac{M}{\tau_r}\right) + \dfrac{\left(k_p - 1\right)}{\delta}\left(\gamma' + \dfrac{1}{\tau_r}\right) \\ l_4 = -\dfrac{\left(k_p - 1\right)}{\delta}\hat{\omega}_r \end{cases} \quad (21)$$

C. The Luenberger Observer Stability Analysis

The characteristic matrix of the observer (*A-LC*) stands for the linear element of the observation error. If the real parts of its poles are negative for any value of the operation speed, the stability of this element will be guaranteed.

Fig. 1 shows the evolution of the system poles and zeros in accordance with the rotor speed.

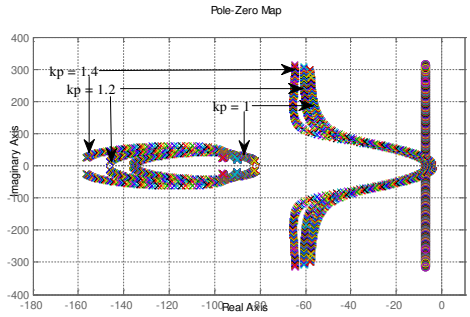


Fig. 2. Evolution of the observer poles and zeros

When we astutely decide on the value k_p, the obsrver stability will be maintained and the dynamic observation wil be faster than the system itself. Moreover, when we examine Fig. 1, , we notice that every speed point has four poles. All these poles are complex conjugates and have a negative real part. But Fig. 2 mirrors the progress of the observer poles and zeros vis a vis the rotor speed and for the various proportionality coefficient values k_p

D. Simultaneous estimation of the rotor speed and stator resistance

When carrying out the operation, the temperature changes. In fact, the changing temperature causes the resistance of both the rotor and the stator to vary. Therefore, the adaptive observer that we suggest can be enlarged to involve the rotor resistance estimation. If we consider the rotor velocity and resistance as unidentified factors of the observer, as the rotor flux are computed from (14) and (15) and are given by this equation .

$$\dot{e} = \left\{\left(A(\bar{\omega}_r) + A(\bar{R}_s)\right) - LC\right\} e(t) - \left(\Delta A(\omega_r) + \Delta A(R_s)\right)\tilde{x}(t) \quad (22)$$

Where $\Delta A(\bar{\omega}_r) = A(\bar{\omega}_r) - A(\omega_r) = \begin{pmatrix} O_2 & -\delta\Delta\omega_r J \\ O_2 & \Delta\omega_r J \end{pmatrix}$;

$$\Delta A_{R_s}(R_s) = A(\bar{R}_s) - A(R_s) = \begin{pmatrix} -\dfrac{\Delta R_s}{\sigma L_s} I_2 & O_2 \\ O_2 & O_2 \end{pmatrix};$$

$\Delta\omega_r = \bar{\omega}_r - \omega_r$ and $\Delta R_s = \bar{R}_s - R_s$.

A Lyapunov function candidate v is identified as:

$$v = e_n^T e_n + \frac{\left(\Delta\omega_r\right)^2}{\lambda} + \frac{\left(\Delta R_s\right)^2}{\lambda'} \quad (23)$$

The time derivative of $\dot{v}$ will be

$$\dot{v} = e^T\left[(A-LC)^T + (A-LC)\right]e - 2\frac{\Delta\omega_r}{\delta}\left(e_{i_{s\alpha}}\bar{\Phi}_{r\beta} - e_{i_{s\beta}}\bar{\Phi}_{r\alpha}\right) + \frac{2}{\lambda}\Delta\omega_r\frac{d\Delta\omega_r}{dt} + \frac{2\Delta R_s}{\sigma L_s}\left(e_{i_{s\beta}}\bar{i}_{s\beta} + e_{i_{s\alpha}}\bar{i}_{s\alpha}\right) + \frac{2}{\lambda'\sigma L_s}\Delta R_s\frac{d\Delta R_s}{dt} \quad (24)$$

The adaptive design for the Simultaneous estimation of the rotor speed and stator resistance is given by:

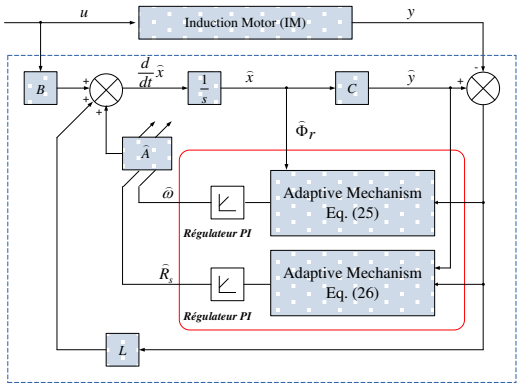


Fig. 3. Structure of a parallel estimator of the rotor speed and the stator resistance.

$$\bar{\omega}_r = K_{P\omega_r}\left(e_{i_{\alpha s}}\bar{\Phi}_{\beta r} - e_{i_{\beta s}}\bar{\Phi}_{\alpha r}\right) + K_{I\omega_r}\int\left(e_{i_{\alpha s}}\bar{\Phi}_{\beta r} - e_{i_{\beta s}}\bar{\Phi}_{\alpha r}\right)dt \quad (25)$$

$$\bar{R}_s = K_{PR_s}\left(e_{i_{\beta s}}\bar{i}_{\beta s} + e_{i_{\alpha s}}\bar{i}_{\alpha s}\right) + K_{IR_s}\int\left(e_{i_{\beta s}}\bar{i}_{\beta s} + e_{i_{\alpha s}}\bar{i}_{\alpha s}\right)dt \quad (26)$$

Fig. 3 is a presentation of the suggested adaptive observer structure for the simultaneous estimation of speed as well as the stator resistance.

IV. Determining the Gains of the Regulators, the Speed Estimators and the Stator Resistance

To underscore the gains of the PI regulators which are used to simultaneously estimate the rotor speed and the stator resistance, one has to allude to the stability study of the control system closed-loop transfer function of the rotor speed and that of the stator resistance [15- 17].

When using the state representation of the asynchronous machine defined by the system equation (14) and that of the observer expressed by the system equation (15), we get to the error-expressions related to the following stator currents and rotor flux:

$$\begin{cases} pe_{i_s} = \left(a_{11} + L\right)e_{i_s} + a_{12}e_{\Phi_r} + \Delta a_{12}\hat{\Phi}_r + \Delta a_{11}\hat{i}_s \\ pe_{\Phi_r} = a_{21}e_{i_s} + \Delta a_{21}\hat{i}_s + a_{22}e_{\Phi_r} + \Delta a_{22}\hat{\Phi}_r \end{cases} \quad (27)$$

With

$$e_{i_s} = i_s - \hat{i}_s \;;\; e_{\Phi_r} = \Phi_r - \hat{\Phi}_r \;;\; \Delta a_{11} = -\frac{\Delta R_s}{\sigma L_s} I_2 \;;$$

$$\Delta a_{12} = -\frac{\Delta\omega}{\delta} J \;;\; \Delta a_{21} = 0 \text{ and } \Delta a_{22} = \Delta\omega_r J \,.$$

It should be noted here that the error on the stator currents is used for the estimation of both the rotor speed and the stator resistance. When substituting the equations of the system (27), we obtain:

$$\begin{cases} \left(pI - \left(a_{11} + L\right)\right)e_{i_s} = a_{12}e_{\Phi_r} + \Delta a_{12}\hat{\Phi}_r + \Delta a_{11}\hat{i}_s \\ \left(pI - a_{22}\right)e_{\Phi} = a_{21}e_{i_s} + \Delta a_{22}\hat{\Phi}_r \end{cases} \quad (28)$$

Therefore, the error on the stator currents can be expressed according to the error on the rotor speed and the error on the stator resistance as:

$$e_{i_s} = e_1 + e_2 \quad (29)$$

With:

$$\begin{cases} e_1 = G_\omega J\hat{\Phi}_r\Delta\omega \\ e_2 = G_{R_s}\hat{i}_s\Delta R_s \end{cases} \quad (30)$$

Where:

$$\begin{cases} G_\omega = \dfrac{p}{\delta}\left[p^2 - p(a_{11} + a_{22} + L) + a_{22}(a_{11} + L + \dfrac{a_{21}}{\delta})\right]^{-1} \\ G_{R_s} = \dfrac{(pI_2 - a_{22})}{\sigma L_s}\left[p^2 - p(a_{11} + a_{22} + L) + a_{22}(a_{11} + L + \dfrac{a_{21}}{\delta})\right]^{-1} \end{cases} \quad (31)$$

By simplifying the equations of the system (31), we get:

$$\begin{cases} G_\omega = \dfrac{p^3 + a_1p^2 + a_3p}{\delta\left[p^4 + (2a_3 + a_1^2 + a_2^2)p^2 + 2(a_1a_3 + a_2a_4)p + (a_3^2 + a_4^2)\right]} \\ G_{R_s} = \dfrac{p^3 + b_1p^2 + b_2p^3 + b_3}{\dfrac{\sigma L_s}{2}\left[p^4 + (2a_3 + a_1^2 + a_2^2)p^2 + 2(a_1a_3 + a_2a_4)p + (a_3^2 + a_4^2)\right]} \end{cases} \quad (32)$$

With:

$$a_1 = \gamma + \frac{1}{\tau_r} - L_1, a_2 = -\left(L_2 + \omega\right),$$

$$a_3 = \left(\frac{1}{\tau_r}\left(\gamma - L_1 - \frac{M}{\delta\tau_r}\right) - L_2\omega\right), a_4 = -\left(\frac{L_2}{\tau_r} + \omega\left(\gamma - \frac{\delta M}{\tau_r} - L_1\right)\right),$$

$$b_1 = \left(a_1 + \frac{1}{\tau_r}\right), b_2 = -\left(a_3 + \frac{a_1}{\tau_r} + a_2\omega\right), b_3 = \left(\frac{a_3}{\tau_r} + a_4\omega\right).$$

To investigate the stability of the closed loop transfer function of the speed estimator and the stator resistance, we must show the gains of the PI regulators of each estimator.

The closed-loop transfer function of the rotor speed control system is given by the following block diagram:

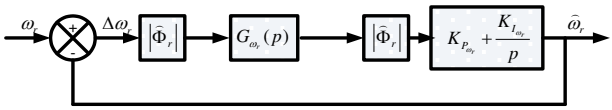
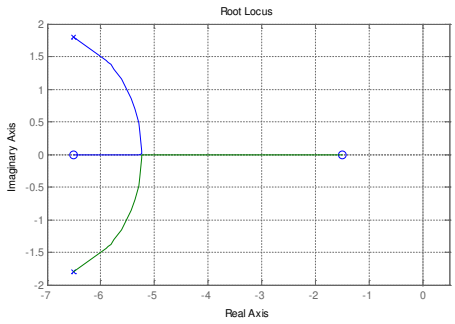
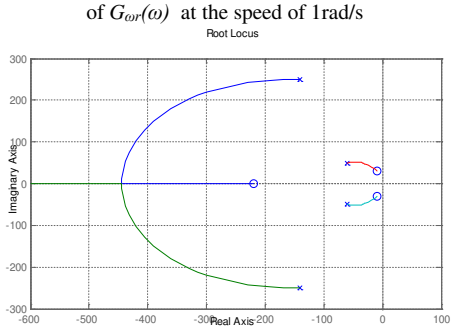


Fig. 4. The control scheme of the speed estimator.

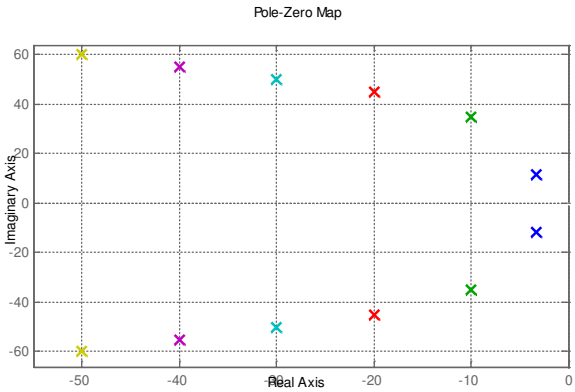
These figures show the locations of the poles and zeros of the transfer function $G_{\omega r}(\omega)$ with respect to the rotor speed:



(a) Location of the dominant poles and zeros of $G_{\omega r}(\omega)$ at the speed of 1rad/s



(b) Location of the poles and zeros of $G_{\omega r}(\omega)$ at the speed of 157 rad/s



(c) Location of the dominant poles of $G_{\omega r}(\omega)$ at various velocities: 157, 125, 75, 50, 25 and 1 rad/s

Fig. 5. Evolutions of the poles and zeros of the transfer function $G_{\omega r}(\omega)$.

For different values of speed, most poles are complex conjugates with a negative real part. Indeed, at the speed of *2 rad/s*, the transfer function $G_{\omega r}(\omega)$ has three zeros of the values: *-1.4*, *-6.3* and *-220*, four complex-conjugate poles of the values: $-6.3 \pm 1.8*j$ and $-240 \pm 11.2*j$.

The dynamics of the speed control system is characterized by the location of the poles of its closed loop transfer function. In fact, to ensure a quick response during the transient conditions and to reduce the steady state noises, the proportional gain $K_{P\omega r}$ is selected high and the ratio ($K_{I\omega r}$/ $K_{P\omega r}$) must be equal to the negative real part of the dominant poles at a given speed. On the basis of the stability study of the closed loop transfer function of the rotor speed control system, we have chosen $K_{P\omega r} = 500$ and $(K_{I\omega r} / K_{P\omega r}) = 6.3$.

The closed loop transfer function of the stator resistance control system is given by the following block diagram:

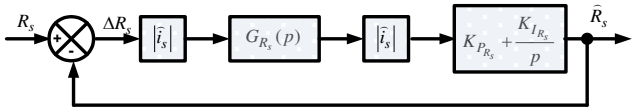


Fig. 6. Scheme for regulating the stator resistance estimator.

For various speed values, the transfer function $G_{Rs}(\omega)$ has three zeros and four complex conjugate poles which lie in the left half-plan of the complex plan.

The location of the dominant poles of the transfer function $G_{Rs}(\omega)$ at a rotational speed of *2 rad/s* is given by the following diagram:

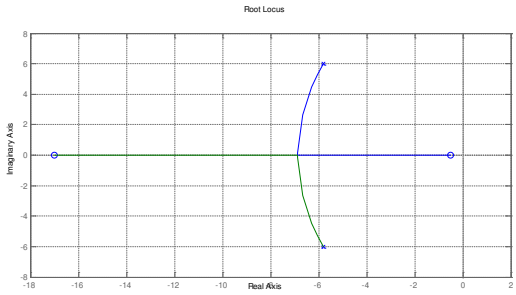


Fig. 7. The location of the dominant poles and zeros of $G_{Rs}(\omega)$ at the speed of 2 rad/s.

To have both a quick response during the transitional schemes and an effective reduction of the steady state noise, the proportional gain K_{PRs} is selected high and the ratio (K_{IRs}/K_{PRs}) must be equal to the negative real part of the dominant poles. On the basis of the stability study of the closed loop transfer function of the stator resistance control system, we have chosen $K_{PRs} = 300$ and $((K_{IRs}/K_{PRs})) = 6.3$.

V. Experimental Results

To validate the performance of the proposed method, a prototype implementation of the sensorless IRFOC of an induction motor drive was carried out. Experimental tests were done based on the estimation scheme for sensorless IRFOC of an induction motor which is proposed in Fig. 8. As a matter of fact, the experimentation has been achieved by using Matlab-Simulink and dSpace DS1104 real time controller board. The experimental setup is composed by squirrel-cage IM a 3Kw, a pulse with modulation (PWM) signals to control the power modules generated by dSpace System, a voltage source inverter (VSI) and a load generated through a magnetic power brake coupled with the three-phase induction motor. What is more, the DC link voltage and stator phase currents and voltages are measured by Hall-type LEM sensors.

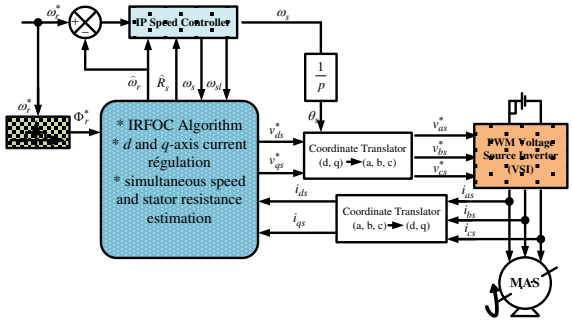
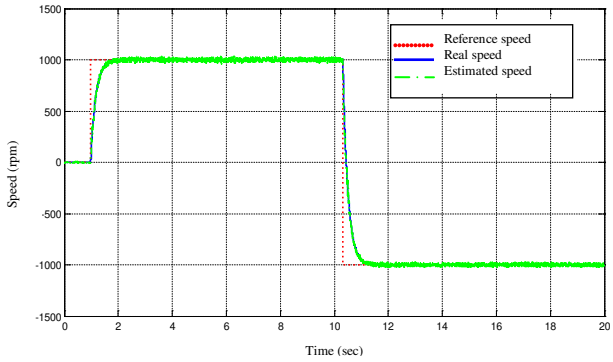
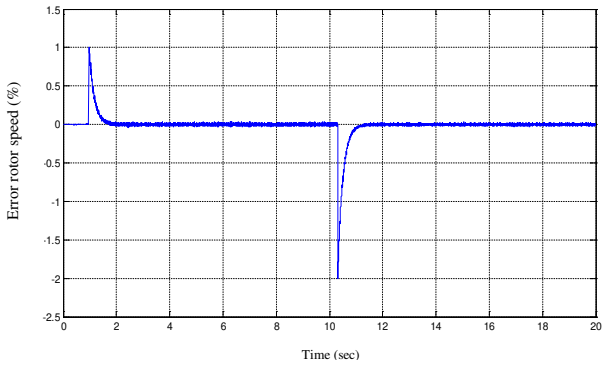


Fig. 8. IRFOC of an asynchronous machine with simultaneous estimation of the rotor speed and the stator resistance.

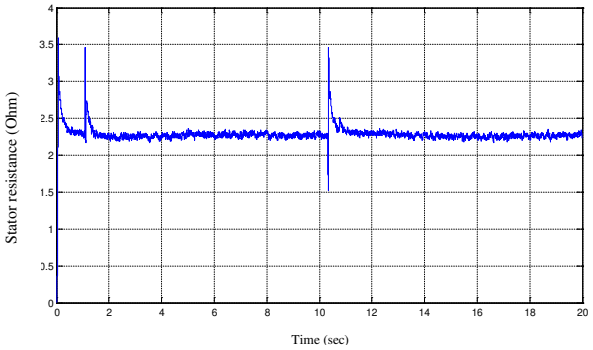
- *The first case*: a preset speed of *1000 rpm* by inverting the rotation direction at the moment *t=10.5s*.



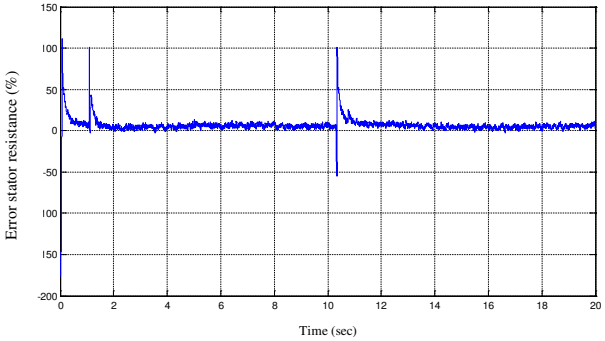
(a) Speed



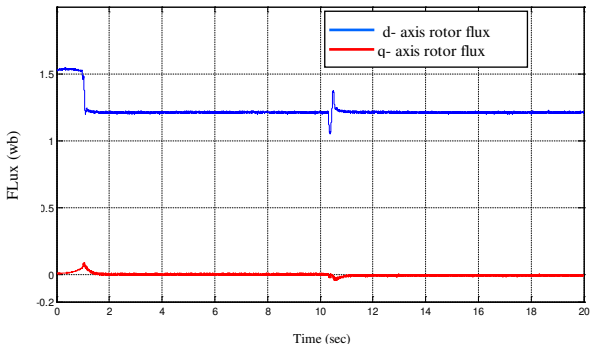
(b) Error rotor speed



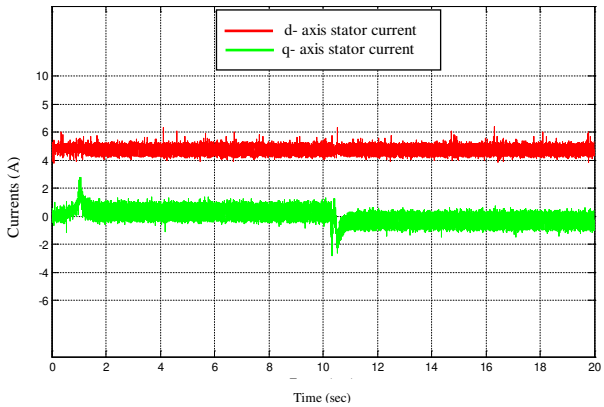
(c) Stator resistance



(d) Error stator resistance



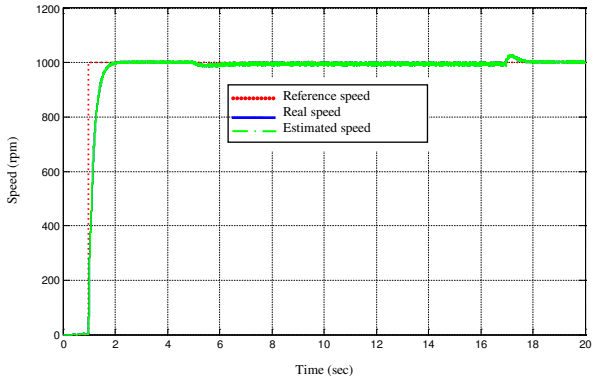
(e) Rotor Flux Φ_{dr} et Φ_{qr}



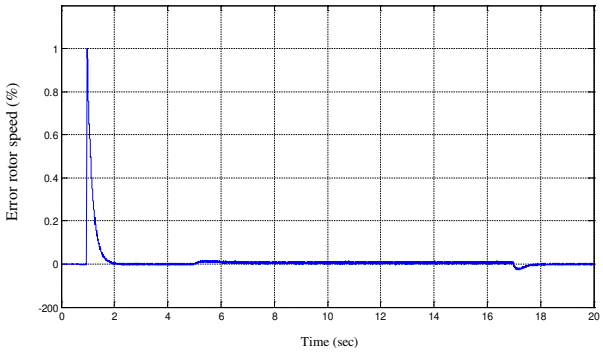
(f) Stator currents i_{ds} et i_{qs}

Fig. 9. Experimental results of the *IRFOC* control without a mechanical sensor through the adaptation of the stator resistance to a speed level of *1000 rpm* and the application of a load torque level.

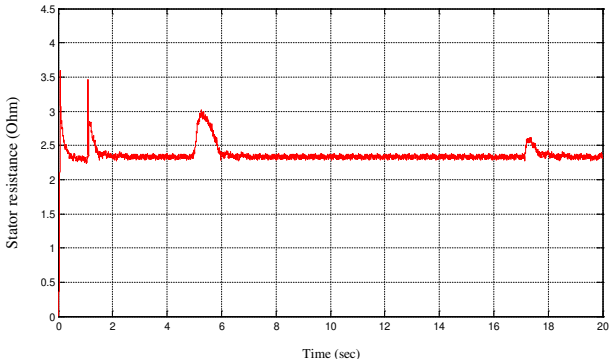
- *The second case*: a preset speed of *1000 rpm*, followed by the application of a load torque equal to *20 Nm* with $t = 5s$, and the abolition of the latter with $t = 17s$.



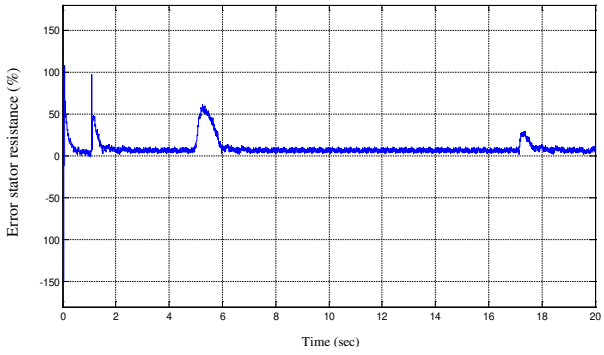
(a) Speed



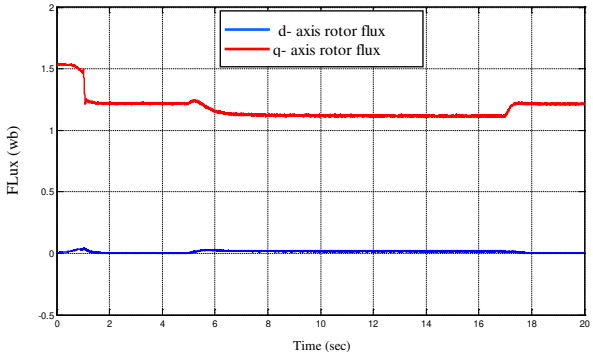
(b) Error speed



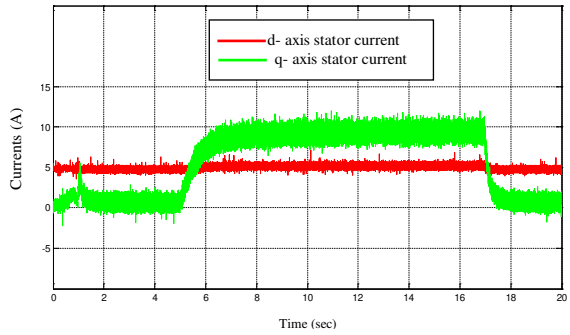
(c) Stator resistance



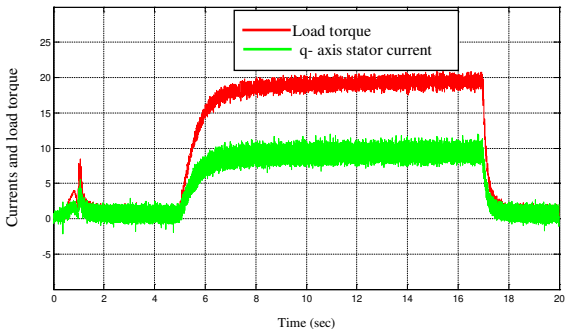
(d) Error stator resistance



(e) Rotor flux



(f) Stator current



(g) Load torque and q-axis stator current

Fig. 5. Simulation results of sensorless IRFOC (with load torque of *20 N.m* applied at *t = 5s*) with the stator resistance tuning the control speed is *1000 rpm.*

For both cases of operation, the stator resistance mechanism estimation is initially halted. The nominal stator resistance is equal to *2.3* Ω, the identification mechanism of the stator resistance is actuated a few seconds after reaching the steady state.

The experimental tests illustrated by the figures (9 (a) and 10 (a)) show that the estimated speed and the actual speed converge to that of the reference. The error between the estimated and the actual sizes is presented by the figures (9 (b) and 10 (b)) and it does not exceed 0.5% in the steady state. The figures (9 (c) and 10 (c)) show the curves of the estimated stator resistance and those of the reference. The convergence of the estimated size of Rs resistance to its reference is proved by the figures (9 (d) and 10 (d) representing the error between the estimated and the actual sizes that do not exceed 2% in the steady state. The guiding principle of the rotor flux is shown by the figures (9 (e) and 10 (e)).

VI. Conclusion

In this paper, stability analysis of simultaneous use of speed and stator resistance estimators for sensorless indirect rotor flux oriented control (IRFOC) induction motor (IM) drives has been presented. It has been concluded that stabilization of each independent speed and stator resistance estimators is insufficient to ensure the stability when used simultaneously. Values of the adaptive PI controller gains of the two estimators based on Root-Locus method have been determined. The validity of all proposed gain selections has been verified and assessed by experimental results.

Appendix

TABLE I. Induction Motor Parameters

Specification		Parameters	
Rated power [kW]	3	R_s [Ω]	2.3
Rated voltage [V]	380	R_r [Ω]	1.83
Rated current [A]	6.6	L_s [H]	0.261
Rated frequency [Hz]	50	L_r [H]	0.261
Number of pole pairs [¯]	2	M [H]	0.245
Rated speed [rpm]	1430	J [Kg.m2]	0.03
		f [Nm.s.rad-1]	0.002

TABLE II. Gains of Different Controller

PI d-q axis current controller		IP speed controller	
k_{ii}	9300	$k_{\omega i}$	6
k_{ip}	29.31	$k_{\omega p}$	0.5

References

[1] F.J. Lin, R.J. Wai, C.H. Lin, D.C. Liu, ‘‘Decoupling stator-flux oriented induction motor drive with uncertain fuzzy neural network observer,’’ *IEEE Trans. Ind. Electron.*, vol. 47, pp. 356–367, Apr. 2000.

[2] S. Suwankawin, S. Sangwongwanich, ‘‘A speed sensorless IM drive with decoupling control and stability analysis of speed estimation,’’ *IEEE Trans. Ind. Electron.*, vol. 49, pp. 444–455, Apr. 2002.

[3] M.N. Uddin, H. Wen, ‘‘Model reference adaptive flux observer based neuro-fuzzy controller for induction motor drive,’’ in *Fourtieth IAS Annual Meeting. Conference Record of the 2005*, *IEEE Industry Applications Conference,* vol. 2, 2005, pp. 1279–1285.

[4] Y Agrebi, Y. Koubaa, M. Boussak, ‘‘Rotor resistance estimation for indirect stator flux oriented induction motor drive based on MRAS scheme,’’ *10th International Conference on Sciences and Techniques of Automatic Control & Computer engineering* STA’2009.

[5] K.B. Mohanty, A. Patra, ‘‘Flux and speed estimation in decoupled induction motor drive using Malman filter,’’ *29th National systems Conference (NSC)*, Dec.2005, pp. 1-9.

[6] M. Barut, S. Bogosyan, M. Gokasan, ‘‘Speed-sensorless estimation for induction motors using extended Kalman filters,’’ *IEEE Trans. Ind. Electron.*, vol. 54, pp. 272–280, Feb. 2007.

[7] A. Goedtel, I.N. Silva, P.J.A. Serni, C.F. Nascimento, ‘‘Neural approach for speed estimation in induction motors,’’ *in 7th International Conference on Intelligent Systems Design and Applications*, (ISDA), 2007, pp. 561–566

[8] A. Meharrar, M. Tioursi, M. Hatti, A.B. Stambouli, ''A variable speed wind generator maximum power tracking based on adaptive neuro-fuzzy inference system,'' *Expert Syst. Appl.*, vol. 38, pp. 7659–7664, 2011.

[9] S. Aloui, T. Maatoug, A. Chaari et Y. Koubaa "Adaptive Observer for MIMO nonlinear systems: Real- time Implementation for an induction Motor " International Journal of Sciences and Techniques of Automatic control & computer engineering IJ-STA, Special Issue, CEM, December 2008, pp.602-611

[10] M. Jouili, K. Jarray, Y. Koubaa and M. Boussak, ''Luenberger state observer for speed sensorless ISFOC induction motor drives,'' *EPSR: Electric Power Systems Research*., vol. 89, pp. 139–147, 2012.

[11] M. Jouili, K. Jarray, Y. Koubaa and M. Boussak, ''Implementation of Sensorless Speed Control for Induction Motor drive Using IRFOC,'' *JES: Journal of Electrical Systems*, vol. 8, pp. 108–118, 2012.

[12] M. Jouili, K. Jarray, Y. Koubaa and M. Boussak, ''A Luenberger State Observer for Simultaneous Estimation of Speed and Rotor Resistance in sensorless Indirect Stator Flux Orientation Control of Induction Motor Drive,'' *IJCSI: International Journal of Computer Science,* vol. 6, 2011, pp. 116–124.

[13] Y. Agrebi, Y. Koubaa, M. Boussak, ''Online Rotor Resistance Estimation Using the Model Reference Adaptive System of Induction Motor,'' *i-manager's Journal of Electrical Engineering*, vol. 3, no 3 Jan./Mar. 2010.

[14] Y. Xing, "A novel rotor resistance identification method for an indirect rotor flux-oriented controlled induction machine systeme", IEEE Transaction on Power Electronics, vol 17, issue. 3, pp. 353-364. 2002.

[15] M. S. Zaky, "A stable adaptive flux observer for a very low speed sensorless induction motor drives insensitive to stator resistance variations", Ain Shams Engineering Journal, production and hosting by Elsevier, pp. 1-10, 17 April 2011

[16] Mechernene, A. M. Zerikat and A. Hachlef, (2008) Fuzzy speed regulation for induction motor associated with field-oriented control, International Journal of Sciences and Techniques of automatic Control and Computer Engineering, IJSTA, Special issue, CEM, pp.516-531.

[17] S. Zaky, "Stability analysis simultaneous estimation of speed and stator resistance for sensorless induction motor drives", Procceddings of the 14th International Middle East Power Systems Conference (MEPCON'10), pp. 364-370, paper ID 180, December 19-21 2010, Cairo University, Egypt.



Mabrouk JOUILI was born in Ben Guerdane, Tunisia, on 14 August 1980. He received the Engineer degree and the M.S. degrees 2005 and 2007, respectively, and the Doctorat theses in 2014 from the National Engineering school of Sfax (ENIS), all in electrical engineering. Since September 2012, he has been an Assistant Professor at the Institut Supérieur des Sciences Appliquées et de Technologie de Gabès (ISSATG), Tunisia. His research is in the areas of electrical machines, sensorless vector control ac motor drives, and advanced digital motion control.



Youssef AGREBI ZORGANI is currently working as an Associate Professor in the Institut Supérieur des Etudes Technologiques de Sfax, Tunisia. He received the B.S degree from the Ecole Normale Supérieure de l'Enseignement Technique de Tunis (ENSET) in 1995 and the master degree in April 2007 from the National Engineering School of Sfax (ENIS), and the Ph.D. degree from National Engineering School of Sfax (ENIS), Tunisia, in 2012 in electrical engineering and the Ph.D. degree from Faculty of Science and Technology Aix-MarseilleIII, France, in 2012 in Automatic. His research interests are the areas of electrical machines, power electronics, motor drives and Renewable energy.



Yassine Koubaa was born in Sfax, Tunisia in 1961. He received the B.S. and DEA (master) degrees in 84 and 86, respectively, the Doctorat theses in 1996, the ''Habilitation Universitaire'' (HDR) from the National Engineering school of Sfax (ENIS) all in electrical engineering. From 1989 to 1996, he was an Assistant professor in the Electrical Engineering Department of ENIS. In september 1997, he has been an Associate Professor. Since September 2005, he becomes a full professor at the same university.

His main research interests cover several aspects related to electrical machines, including systems identification, advanced motion control and diagnostics. He has authored more than 70 papers in international conferences and technical journals in the area as well as many patents. He serves as a member of the Scientific and the Technical Program Committees of several international conferences and technical journals in the motor drives fields.

Professor Yassine Koubaa is the head of Automatic Control Research Laboratory (Sfax-Tunisia) and the editor in chief of International Journal on Sciences and Techniques of Automatic control & computer engineering (IJ-STA).



Mohamed Boussak was born in El Haouaria, Tunisia, on 28 December 1958. He received the B.S. and D.E.A. degrees from Ecole Normale Supérieure de l'Enseignement Technique de Tunis, Tunis, Tunisia, in 1983 and 1985, respectively, the Ph.D. degree from Pierre et Marie Curie University, Paris, France, in 1989, and the Habilitation à Diriger des Recherches from Aix-Marseille III University, Marseille, France, in 2004, all in electrical engineering. He was a Researcher with Ecole Supérieure d'Ingénieurs de Marseille (ESIM) from 1989 to 1990. Between 1990 and 1991, he was a Research Teacher of electrical engineering with Claude Bernard University, Lyon, France. From 1991 to 2004, he was an Associate Professor with ESIM. From 2004 to 2008, he was an Associate Professor of electrical machines with Ecole Centrale Marseille, Marseille, where he has been a Senior Professor since 2009. He has published more than 150 papers on top rank international journals and refereed conferences. His current research interests include electrical machines, power conversion systems, sensorless vector control ac motor drives, advanced digital motion control, diagnosis faults, and fault tolerant control. Dr. Boussak is currently serves as a member of the technical program committees of several international conferences and scientific journals in the areas of power electronics and motor drives fields. He is a member of the IEEE Industry Application, the IEEE Industrial Electronics, and the IEEE Power Electronics Societies.